Title

From intentions to actions: Neural oscillations encode motor processes through phase, amplitude and phase-amplitude coupling

Authors

Etienne Combrisson[1,2,3], Marcela Perrone-Bertolotti[4], Juan LP Soto[5], Golnoush Alamian[1], Philippe Kahane[4], J-P Lachaux[3], Aymeric Guillot[2], Karim Jerbi[1]

Affiliations

[1] Psychology Department, University of Montreal, QC, Canada
[2] Center of Research and Innovation in Sport, Mental Processes and Motor Performance, University Claude Bernard Lyon I, University of Lyon, Villeurbanne, France
[3] Lyon Neuroscience Research Center, Brain Dynamics and Cognition, INSERM U1028, UMR 5292, Lyon University
[4] Neurology Dept and GIN U836 INSERM-UJF-CEA, Grenoble University Hospital, Grenoble, France
[5] Telecommunications and Control Engineering Department, University of Sao Paulo, Sao Paulo, Brazil

Corresponding author

Etienne Combrisson
Address:
Psychology Department
University of Montreal
Pavillon Marie-Victorin
90, avenue Vincent d'Indy, Quebec, Canada
E-mail address: e.combrisson@gmail.com

List of potential referees (For cover letter):

Andrea Brovelli
Julien Voisin
Nikolai Axmacher
Michel Le van Quyen
Lauri Parkkonnen
Nathan Crone
Andrea Greggoriu
Joachim Gross
Paolo Belardinelli
Hyojin Park
Felix Darvas
Tonio Ball

ABSTRACT

Goal-directed motor behavior is associated with changes in patterns of rhythmic neuronal activity across widely distributed brain areas. In particular, movement initiation and execution is mediated by patterns of synchronization and desynchronization that occur concurrently across distinct frequency bands and in multiple motor cortical areas. To date, motor-related local oscillatory modulations are predominantly examined by quantifying increases or suppressions in spectral power. However, beyond signal power, further spectral properties such as phase and phase-amplitude coupling (PAC) have also been shown to carry information with regards to the oscillatory dynamics underlying motor processes. The distinct functional roles of phase, amplitude and PAC across planning and execution of goal-directed motor behavior remain largely elusive. Here, we address this question with unprecedented resolution thanks to rare multi-site intracerebral EEG recordings in human subjects performing a delayed motor task. To compare the roles of phase, amplitude and PAC in motor planning and execution, task-related modulations of electrophysiological brain signals were monitored at movement execution and during the delay period where motor intention is present but execution is withheld. In particular, we used a machine-learning framework to identify the key contributions of the various neuronal responses. We found a high degree of overlap between the brain network patterns observed during planning and execution. Prominent amplitude increases in the delta (2-4 Hz) and high gamma (60-200 Hz) bands were observed during planning and execution. In contrast, motor alpha (8-13 Hz) and beta (13-30 Hz) power were suppressed during execution, but enhanced during the delay period. Interestingly, single-trial classification revealed that low-frequency phase information was the most discriminant feature in dissociating action from intention. Additionally, despite providing weaker decoding, PAC features led to statistically significant classification of motor states, particularly in anterior cingulate cortex and premotor brain areas. These results advance our understanding of the distinct and partly overlapping involvement of phase, amplitude and PAC in the neuronal mechanisms underlying motor intentions and executions.

Keywords

Neural oscillations, motor intention, motor planning, phase, phase-amplitude coupling, intracranial EEG

1 Introduction

The simplest motor act, such as stretching out your arm to grasp a cup of coffee, is mediated by a rich and complex chain of neuronal processes. What in essence may seem as the realization of a straightforward motor command is in fact carried out by a cascade of events ranging from action selection and planning to motor execution and monitoring. The neural mechanisms that mediate the transformation of intentions into actions have been the subject of a thriving body of research for decades (Ariani et al., 2015; Brovelli et al., 2005; Desmurget and Sirigu, 2009; Jeannerod, 1994; Kalaska, 2009; Lau, 2004; Paus, 2001; Schwartz, 2016; Snyder et al., 1997). However, because the neuronal processes at play can be observed at various spatial scales and with different recording techniques, parallel streams of research have given rise to a rich but fragmented understanding of the local and large-scale integrative electrophysiological mechanisms involved in motor control.

Both human and non-human primate research provides solid evidence that goal-directed motor behavior is associated with changes in patterns of rhythmic neuronal activity across widely distributed brain areas (Schnitzler and Gross, 2005). Movement initiation and execution is mediated by patterns of synchronization and desynchronization that occur concurrently across distinct frequency bands and in multiple motor cortical areas (Cheyne et al., 2008; Jurkiewicz et al., 2006; Pfurtscheller et al., 2003; Saleh et al., 2010)

To date, motor-related local oscillatory modulations are by and large examined by quantifying increases or suppressions in spectral power (Cheyne et al., 2008; Jurkiewicz et al., 2006; Pfurtscheller et al., 2003; Saleh et al., 2010). However, beyond band-limited oscillatory power, other spectral properties, namely phase and phase-amplitude coupling (PAC), are also thought to play a key role in neuronal encoding and information processing. The involvement of phase information in neuronal encoding has been extensively investigated in numerous perceptual modalities and higher-order cognitive tasks (Drewes and VanRullen, 2011; Dugue et al., 2011; Jensen et al., 2014; Klimesch et al., 2008, 2007; Montemurro et al., 2008; Palva and Palva, 2007; Sauseng and Klimesch, 2008; Sherman et al., 2016; VanRullen et al., 2011). In comparison, the role of phase and phase-based measures in the neuronal mechanisms that mediate motor processes is still under-investigated. Interestingly, a few studies provide evidence for the involvement of low-frequency phase and amplitude in the neuronal encoding of movement parameters (Hammer et al., 2016, 2013; Jerbi et al., 2011, 2007; Milekovic et al., 2012; Miller et al., 2012; Waldert et al., 2009, 2008). Nevertheless, the spatial, temporal and spectral dynamics of putative phase coding across the chain of processes starting from goal encoding, to motor planning and motor command execution, are still largely unresolved.

Furthermore, recent years have witnessed a surge in the interest in the putative mechanistic function of PAC (Cohen et al., 2008; Hemptinne et al., 2013; Lee and Jeong, 2013; Newman et al., 2013; Voytek, 2010, Bahramisharif et al., 2013) and numerous measures of PAC have been proposed (Canolty, 2006; Nakhnikian et al., 2016; Tort et al., 2010; Voytek et al., 2013, Ozkurt, 2012). Conceptually, PAC may provide a flexible framework for information processing by means of cross-frequency synchronization (Canolty and Knight, n.d.; Hyafil et al., 2015). However, despite important advances (Hemptinne et al., 2013; Özkurt and Schnitzler, 2011; Soto and Jerbi, 2012; Yanagisawa et al., 2012), the precise role of PAC in mediating motor planning and execution is still an open question. More specifically, the distinct functional role and mechanistic links between phase, amplitude and PAC estimates during motor behavior remain largely elusive.

Here, we compare the involvement of all three measures with high spatial, spectral and temporal resolution via access to rare multi-site intracerebral depth electrode recordings in humans performing a delayed motor task. In particular, we monitored modulations of neural activity at movement execution but also during the delay time window where motor intention is present but execution is withheld. In addition, we used a machine-learning approach to identify the key contributions and differences between the various neuronal responses. We found a high degree of overlap between power modulations patterns in the planning and execution periods, with prominent increases in the delta (2-4 Hz) and high gamma (60-200 Hz) bands. Alpha (8-13 Hz) and beta (13-30 Hz) power as well as very low-frequency phase parameters (<1,5 Hz) were the most discriminant features in dissociating action from intention. Despite providing weaker decoding, PAC features led to statistically significant classification of motor states, particularly in premotor brain areas. These results advance our understanding of the distinct and partly overlapping involvement of phase, amplitude and PAC in the neuronal mechanisms underlying motor intentions and executions.

2 Material and methods

2.1 Participants

Six patients with intractable epilepsy participated in this study (6 females, mean age 22.17±4.6). The patients were stereotactically implanted with multi-lead EEG depth electrodes at the Epilepsy Department of the Grenoble Neurological Hospital (Grenoble, France). In collaboration with the medical staff and based on visual inspection, electrodes presenting pathological waveforms were discarded from the present study. All participants provided written informed consent, and the experimental procedures were approved by the Institutional Review Board and by the National French Science Ethical Committee. Patient-specific clinical details are provided in Table 1.

2.2 Electrode implantation and Stereotactic EEG recordings

Each patient was implanted with stereotactic electroencephalography (SEEG) electrodes. Each one of them has a diameter of 0.8 mm and, depending on the implanted structure, composed with 10 to 15 contacts of 2 mm wide and 1.5 mm apart (DIXI Medical Instrument). Intracranial EEG signals were recorded from a total of 748 intracerebral sites across all patients (126 sites in each participant, except for one patient who had 118 recording sites). At the time of acquisition, a white matter electrode was used as reference and data were bandpass filtered from 0.1 to 200 Hz and sampled at 1024 Hz. Electrode locations were determined using the stereotactic implantation scheme and the Talairach and Tournoux proportional atlas (Talairach and Tournoux, 1993). The electrodes were localized in each individual subject in Talairach coordinates (based on post-implantation CT) and then a transformation to standard MNI coordinate system was performed according to standard routines and previously reported procedures (Bastin et al., 2016; Jerbi et al., 2010, 2009; Ossandon et al., 2011).

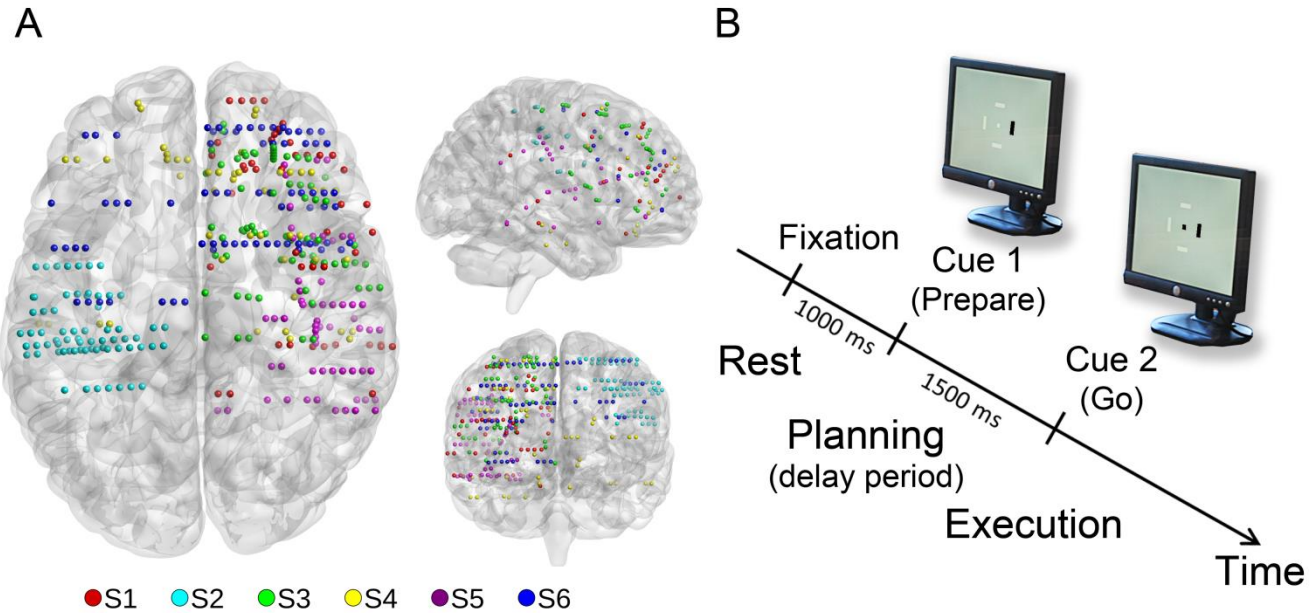

Figure 1. Delayed center-out task definition and Implantation visualization for the 6 subjects on a 3-D standard (MNI) brain *A*, Depth electrodes representation on a top, right and frontal view. We used one color pear subject *B*, Design of the delayed motor task where the direction of the movement is instructed at Cue1, and the actual movement in carried out at Cue 2 ('Go signal'). The timeline consists of three periods: Rest, a delay period (motor planning/intention) and movement execution.

2.3 Delayed center-out motor task

After a rest period of 1000ms, the participants were visually cued to to prepare a movement towards a visually presented target in one of four possible directions: up, down, left or right (*Planning phase*). Next, after a 1500 ms delay period, a Go signal prompted the subjects to move the cursor towards the target (*Execution Phase*). The Go signal consisted of a central cue changing from white to black. Figure 1c shows the task design.

	Handedness	Age	Gender	Epilepsy
P1	D	19	F	Frontal lobe (RH)
P2	D	23	F	Frontal lobe (LH)
P3	D	18	F	Frontal lobe (RH)
P4	D	18	F	Frontal lobe (RH)
P5	D	31	F	Insular (RH)
P6	D	24	F	Frontal lobe (LH)

Table 1. Patient data: age, gender, and broad description of epilepsy type as determined by the clinical staff of the Grenoble Neurological Hospital, Grenoble, France (Recording sites with epileptogenic activity were excluded from the analyses).

2.4 Data preprocessing

SEEG data preprocessing was conducted according to our routine procedures (Bastin et al., 2016; Jerbi et al., 2009). These include signal bipolarization where each electrode site is re-referenced to its direct neighbor. Bipolar re-referencing can increase sensitivity and reduce artefacts by canceling out distant signals that are picked up by adjacent electrode contacts (e.g. mains power). The spatial resolution of bipolar SEEG with the electrodes used here is approximately 3 mm (Jerbi et al., 2009; Kahane et al., 2006; Lachaux et al., 2003). Next, using visual inspection and time-frequency explorations of the signal we exclude electrodes containing pathological epileptic activity. In addition, electrodes located close to the extra-ocular eye muscles were systematically excluded to avoid contaminating our analyses with eye-movement activity. The pre-processing led to a total of 583 bipolar derivations across all participants.

2.5 Spectral analyses

We investigated phase, power and phase-amplitude coupling in several standard frequency bands defined as follow: very low frequency component (VLFC) [0.1-1.5Hz], delta (δ) [2-4Hz], theta (θ) [5-7Hz], alpha (α) [8-13Hz], beta (β) [13-30Hz], low gamma (low γ) [30-60] and broadband gamma (high γ) [60-200Hz]. The power features were computed in six bands (δ, θ, α, β, low γ and high γ), while the phase features were extracted for 4 bands (VLFC, δ, θ and α) and the phase-amplitude coupling was extracted using three combinations (δ, θ and α for phase and high γ for amplitude). In total 13 features were extracted for each SEEG bipolar derivation.

2.5.1 Spectral power estimation

Band-specific power modulations were computed using the Hilbert transform: we first filtered the data segments corresponding to each trial in the required band using a two-way least-squares FIR filter in order to avoid phase-shifting. We then computed the Hilbert transform of the filtered signal and calculated power by taking the square of the amplitude component (envelope). For the specific case of high-gamma, we split the 60-200Hz range into multiple non-overlapping10 Hz bands. As

performed in our previous studies, the broadband gamma power is then obtained by taking the mean of all of the successive 10Hz-wide normalized bands (Jerbi et al., 2009; Ossandon et al., 2011, Bastin et al., 2016). Comparable power estimations were obtained when using a wavelet approach (Tallon-Baudry et al., 1996) (Morlet wavelets) but we deliberately chose to use the Hilbert-based power computation to have a homogeneous methodological framework across all three features, since the Hilbert method was used to assess phase and PAC features (see below).
Statistical evaluation of tasked-based power modulations: Mapping power modulations on the standard MNI brain, is achieved using significant normalized power. The baseline period was defined as a 500 ms time window during pre-stimulus rest (from -750 ms to -250ms). The power in each frequency band was normalized by computing the relative change compared to this baseline at the same frequency (i.e. subtracting then dividing by the mean of the baseline).
Significant power modulations were obtained by standard permutation tests where power values (across time and frequency) during the task are randomly permuted with the corresponding value during baseline. A total of 1000 permutations were performed yielding a null distribution for the relative power which provides a minimal p value of 0.001.

2.5.2 Phase estimation

To extract phase features in a given frequency band, we first apply a bandpass filter to the bipolarized signals. Next, we extract the angle of the complex time-series based on the Hilbert transform. This gives the instantaneous phase for all time points. For the sake of decoding we used a phase value every 250 ms. This was done to have the same temporal resolution across all features (Power features are computed in 500 ms windows with a 50% overlap).
*Statistical evaluation of tasked-based phase modulations: w*e used Rayleigh's test to compute significant phase modulations (Babiloni et al., 2002; Lakatos, 2005; Tallon-Baudry et al., 1996) using the circular statistics toolbox (Berens and others, 2009).

2.5.3 Phase-Amplitude Coupling (PAC) estimation

Different methods for the estimation of PAC are used in the literature (Jensen and Colgin, 2007; Canolty and Knight, 2010; Tort et al., 2010; Soto and Jerbi, 2012; Aru et al., 2015). In order to choose which method to apply here, we first simulated synthetic PAC signals (e.g. Tort et al., 2010) and tested the behavior of several methods, namely Mean Vector Length (MVL) (Canolty, 2006), the Height-Ratio (HR) (Lakatos, 2005), Kullback-Leiber divergence (Tort et al., 2010), normalized direct PAC (ndPAC) (Ozkurt, 2012). We found that the tested PAC methods generally provided very comparable results. The slight differences arose from applying different normalization/surrogate data procedures. Based on this, we chose to use the MVL method combined with a normalization method where the surrogate values were calculated by randomly swapping phase and amplitude across trials (cf. Tort et al., 2010). In short, the PAC estimation procedure applied here can be summarized as follows: First, the low-frequency phase and high-frequency amplitude signals are obtained by filtering and Hilbert transformation in the frequencies of interest (Canolty et al. 2006). Being frequency-dependent, the optimal filter orders were adapted separately for the phase of the slower oscillations (3 cycles used) and for the amplitude of the faster oscillations (6 cycles), as proposed in previous studies (e.g. Bahramisharif et al., 2013). Next, surrogate data are generated by randomly swapping the phase trial data and amplitude trial data (i.e. randomly associating the high frequency amplitude envelope of a trial with the low-frequency phase time course of another trial). This was repeated 1000 times. Then, the normalized PAC value is then obtained by normalizing the MVL by the surrogate data yielding a z-score.

To visualize the emergence of PAC we used a combination of methods: (a) phase-alignment of single-trial TF maps (Canolty, 2006; Hemptinne et al., 2013), (b) a comodulogram (e.g. Foster and Parvizi, 2012; Pittman-Polletta et al., 2014) and (c) Event Related Phase-Amplitude Coupling

(Voytek et al., 2013). When computing the comodulogram, we used the entire planning and execution periods (1500 ms for each) in order to maximize the per-trial number of oscillation cycles for PAC estimation.

Statistical evaluation of tasked-based PAC modulations: The statistical assessment of PAC was achieved by comparing the true PAC values to the null distribution of PAC values computed using surrogate data, i.e. random shuffling across trials of phase and amplitude signals (Tort et al. 2010). A real PAC value that is higher than the 999^{th} highest PAC value obtained with surrogate data, is considered significant at $p<0.001$.

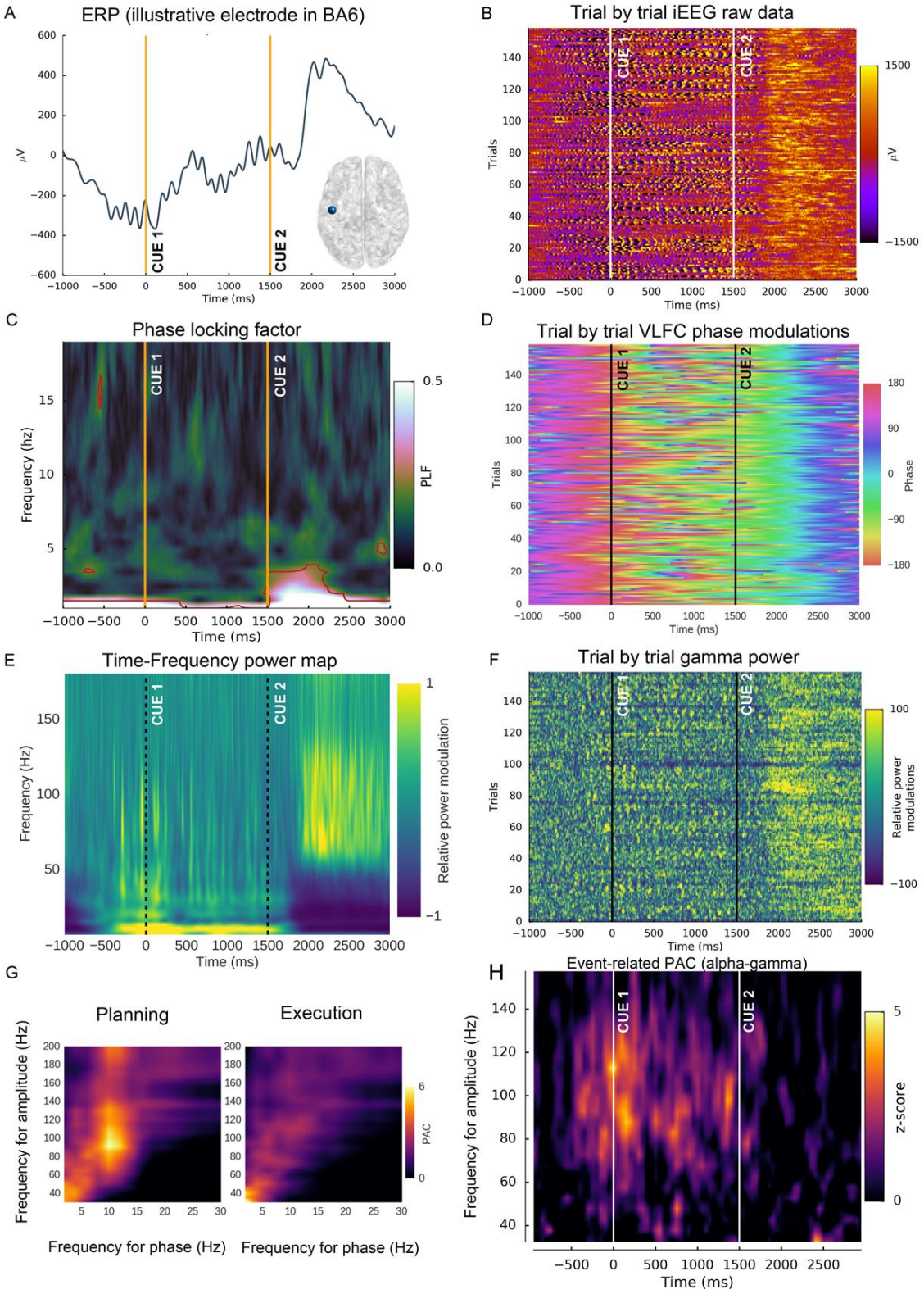

Figure 2. Oscillatory feature extractions from intracranial EEG signals shown for an illustrative electrode in human premotor cortex (BA6). (A) Event-related potential (ERP) across the experiment timeline and anatomical location of the electrode. (B) Trial-by-trial raw iEEG signals. (C) Phase-locking factor indicating stimulus phase-locking (D) Single-trial phase shown here for the VLFC (<1.5 Hz) frequency range. (E) Time-Frequency representation. (F) Trial-by-trial broadband gamma envelopes (Hilbert amplitude, 60-200 Hz). (G) Phase-amplitude coupling maps during planning and during execution revealing prominent alpha-gamma coupling present during planning but absent during execution. (H) Event-related PAC depicts for the same electrode the time course of alpha-Gamma PAC.

2.6 Signal classification

We set out to explore the feasibility of using multi-site human LFP data (583 bipolar electrode sites) to perform three types of motor-state classifications: (a) during execution vs rest, (b) intention vs rest, and (c) execution vs intention. We compared the performance of several classification algorithms (Linear Discriminant Analysis (LDA), Naïve Bayes (NB), k-th Nearest Neighbor (KNN), Support Vector Machine (SVM) with linear and Radial Basis Function kernels and Random Forest). For single features classification, LDA, NB and SVM all provided similar results. We chose to use the LDA approach for its speed, which is a particularly important advantage here given that classifier performance was evaluated using computationally demanding permutation tests.

2.7 Decoding accuracy and statistical evaluation of decoding performance

Classification performance was evaluated using standard stratified 10-fold cross-validation. Here, the data set is first pseudo-randomly split into 10 equally sized observations: 9 segments are used for training the classifier and the last one as test set. This procedure is repeated 10 times so that every observation in the data is used exactly once for testing and at least once for training, but never at the same time. This strict separation of training and testing is critical to ensure the test data are naïve and do not violate basic classification principles (Lemm et al., 2011). The use of stratification seeks to ensure that the relative proportion of labels (or classes) in the whole data set is reasonably preserved within each of the segments after the split. The above procedure was repeated 10 times to reduce the effect of the random generation of the folds, yielding a 10 times 10-fold cross-validation framework. The performance of the achieved decoding is then calculated using the decoding accuracy (DA) metric, which is computed as the mean correct classification across all folds. Although the use of theoretical chance-levels (e.g. DA=50% for binary classification) can provide some useful indication on classifier performance in the presence of a high number of observations, the use of statistics is mandatory in order to assess the significance of classification performance (Combrisson and Jerbi, 2015). To this end, we used a permutation testing framework where the cross-validation and DA calculation are recomputed after randomly shuffling the labels of the classes. For each site and for each type of feature (i.e. power, phase and phase-amplitude coupling) 1000 permutations were generated, which allowed for statistical assessments with p values as lows as 0.001 (Combrisson and Jerbi, 2015; Ojala and Garriga, 2010, Golland and Fischl, 2003; Meyers and Kreiman, 2012).

2.8 Data mapping to a 3-D standard cortical representation

To facilitate the interpretation of the results, all significant task-based feature modulations and decoding results were remapped from the intracranial electrode sites onto a standard cortical representation. To achieve this, all electrode coordinates are first transformed from individual Talairach space to standard MNI space, and custom Matlab code was written to project the data from SEEG sites onto the cortical surface. In practice, data from the iEEG electrodes were assigned to the vertices on the MNI cortical mesh that fell within a fixed radial distance (here 10 mm) from each electrode. This cortical representation technique is methodologically consistent with methods used in previous iEEG studies (Bastin et al., 2016; Jerbi et al., 2009; Ossandon et al., 2012). In addition to generating brain-wide visualization of all significant features and decoding performances, this method can also be used to display the cortical coverage provided by all electrodes in this study (dark grey areas in Figure 2A).

3 Results

The frequency domain analysis of the over 500 intracranial recording sites across all participants revealed that the delayed motor task is mediated by complex patterns of spectral modulations across widely distributed brain areas. Figure 2 illustrates task-related modulations of amplitude, phase and phase-amplitude coupling measured via a recording site in premotor cortex (BA6) in one participant. The ERP and single-trial raw iEEG recordings for this electrode are shown in panels 2A and 2B respectively. Panels 2C and 2D depict the phase-locking factor and a trial-by-trial phase representation across time. The illustrative time-frequency map (Fig 2E) depicts a typical power modulation pattern where movement execution is associated with a strong increase in broadband gamma power and simultaneous power suppression in the alpha, beta and low gamma frequency bands. The delay period (between Cue1 and Cue2) at this site showed a different pattern with power increases at slow frequencies in the delta to alpha range. Because of the high SNR of the intracranial EEG recordings used, it is possible to estimate broadband gamma (60-200 Hz) power on a trial-by-trial basis (Fig 2F). The PAC maps in Figure 2G illustrate the changes in PAC values for the same recording site across motor planning and execution. A peak in PAC between alpha phase and high gamma amplitude is observed during the pre-movement delay period but vanishes during execution, where the maximum PAC is seen between delta phase and low-gamma amplitude. The predominance of the alpha-gamma coupling in the delay period can also confirmed when the TF maps are computed by first realigning the single-trial TF maps to alpha phase in the vicinity of the cue (Figure not shown). Finally, time-resolved event-related PAC estimations (Fig 2H) illustrate the existence at this location of an alpha-gamma coupling specific to the delay period. These oscillatory feature estimations were primarily presented to illustrate the wide variety and high signal-to-noise ratio (SNR) of the features explored in this study, using averaging over trials and, most importantly, in trial-by-trial mode. In the following we discuss the global results obtained using the data from all participants. First we describe the task-based oscillatory modulations and then we examine the results of the data-mining approach.

3.1 Task-based Spectral power modulations

The cortical mapping of power modulations during the delay period and motor execution reveal distinct patterns of increases and decreases across the various frequency bands (Figure 3). As one would expect from previous invasive reports in humans (Crone, 1998a,b; Crone et al., 2006; Babiloni et al., 2016; Bundy et al., 2016; Rektor et al., 2006), our results confirm motor execution is associated with prominent suppressions of alpha/mu and beta band power and with increases in high gamma power, all occurring primarily in motor and premotor cortices. The power modulations shown in figure 3, also indicate significant task-based modulations beyond these areas, extending to parietal, prefrontal and cingulate areas. When comparing the brain-wide significant power changes for both planning and execution, we first see the large degree of overlap between the statistically significantly active areas in both conditions. Second, two distinct patterns seem to emerge when we consider the direction of the effects across frequency bands: The alpha, beta and low-gamma bands show a reversal of the effect from a significant increase during planning to a significant suppression during execution. By contrast, the remaining bands (delta, theta and high gamma) all show a consistent significant power increase both during the planning and execution periods, although the effect is stronger at execution. It is noteworthy that the high gamma increase was prominent over multiple frontal and prefrontal brain areas bilaterally, with strong peaks in motor and premotor cortices during execution. Most of these areas also showed a significant increase of power above baseline levels during the delay period, potentially related to movement goal-encoding and motor planning processes.

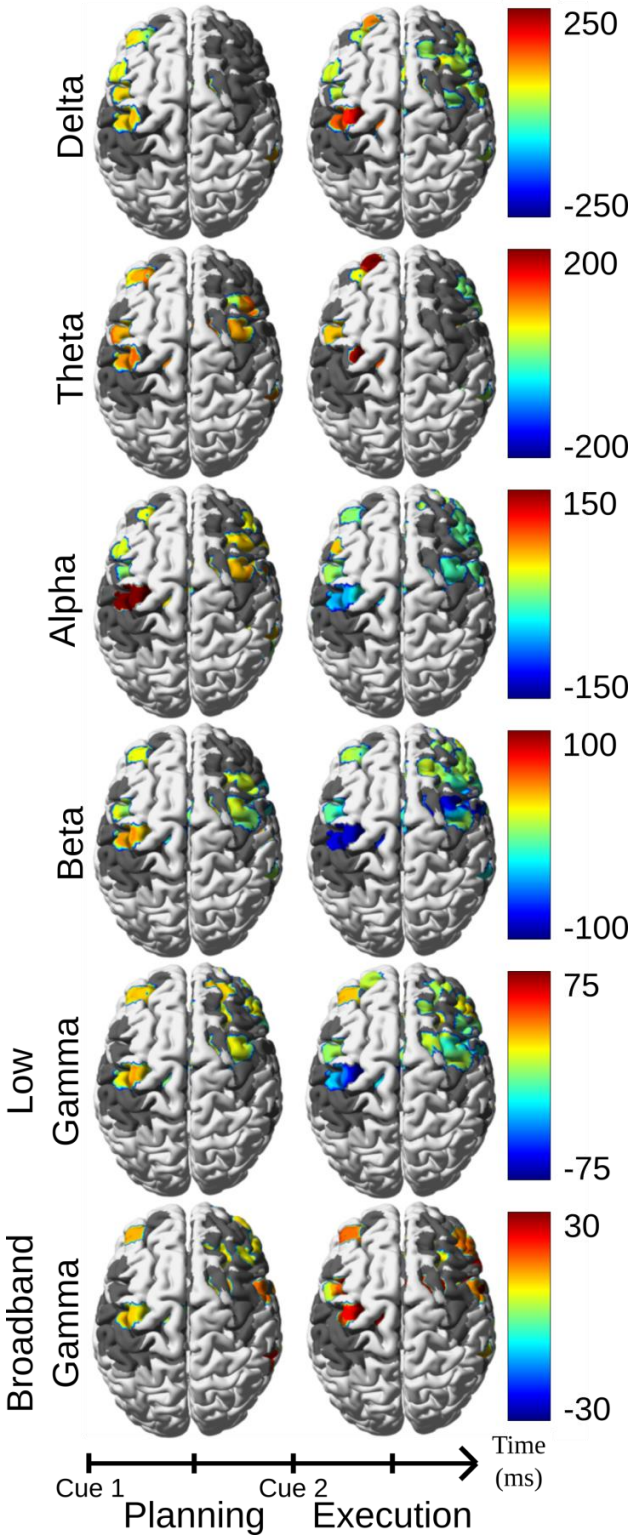

Figure 3. Task-related modulations of spectral power during planning and execution of upper limb movements. The color bars represent percent relative changes (%) of power during planning (250-750ms) and during execution (2000-2500ms) with respect to baseline power during pre-stimulus rest (-750 to -250ms). The power modulations are shown for delta (2-4Hz), theta (5-7Hz), alpha (8-13Hz), beta (13-30Hz), low gamma (30-60Hz) and broadband gamma (60-200Hz). All modulations shown are statistically significant (permutation tests, $p<0.05$, FDR-corrected). Dark grey areas represent cortical regions for which electrode coverage was available but where the modulations did not reach statistical significance.

3.2 Task-based Phase modulations

The patterns of statistically significant changes in phase across all frequency bands show a predominant effect in the lower frequencies (Figure 4). In particular, the VLFC range (i.e. <1.5 Hz) shows consistent phase values in motor cortex with a reversal in sign between the selected instants in planning and execution windows. Interestingly, in addition to being sparser, consistent phase effects in the theta and alpha range were found in prefrontal areas. The significant delta phase angle over primary motor cortex during execution is in line with previous reports of delta-range coupling between motor cortex and movement parameters (Jerbi et al., 2007). Dark grey areas show the regions for which data were available but which did not exceed the significance threshold (Rayleigh test).

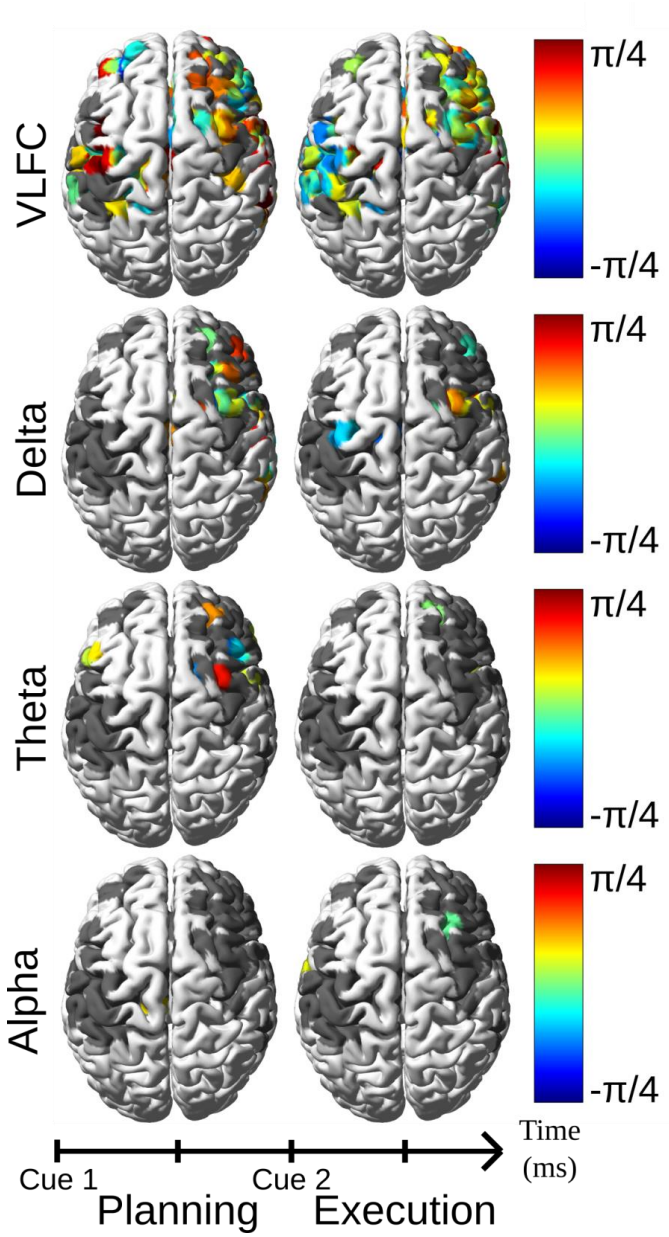

Figure 4. Task-related modulations of instantaneous phase during planning and execution of upper limb movements. The color bars represent mean phase computed at 500 ms (planning) and at 2250 ms (execution), which corresponds to the centers of the windows used for power (Fig 3). Phase modulations were computed for very low frequency component (VLFC) (<1.5 Hz), delta (2-4Hz), theta (5-7Hz) and alpha (8-13Hz) bands. All modulations shown are statistically significant (Rayleigh's test based on the circular statistics toolbox (Berens et al. (2009), $p<0.001$). Dark grey areas represent cortical regions for which electrode coverage was available but where the modulations did not reach statistical significance.

3.3 Task-based PAC modulations

Statistically significant levels of phase-amplitude coupling were found in multiple brain areas and with very similar distributions at execution and during the delay period in the absence of movement (Figure 5). In fact, our results suggest higher PAC during the goal-encoding and planning phase than during movement execution. The most prominent PAC effects in primary motor cortex were obtained for alpha-gamma interactions, but were only present during the planning period. This M1 alpha-gamma PAC virtually disappears at the time of execution. Interestingly, it is replaced by M1 delta-gamma PAC during motor execution. In addition, as shown in the right panel of Figure 5, depth recordings in the medial wall also reveal statistically significant PAC in ACC (cingulate motor cortex, CMA BA32) and in medial premotor areas (SMA, BA6) for all three slow frequency phase ranges explored (delta, theta and alpha). These PAC modulations are likely to reflect the involvement of SMA and cingulate motor areas in action selection, planning, execution as well as inhibition.

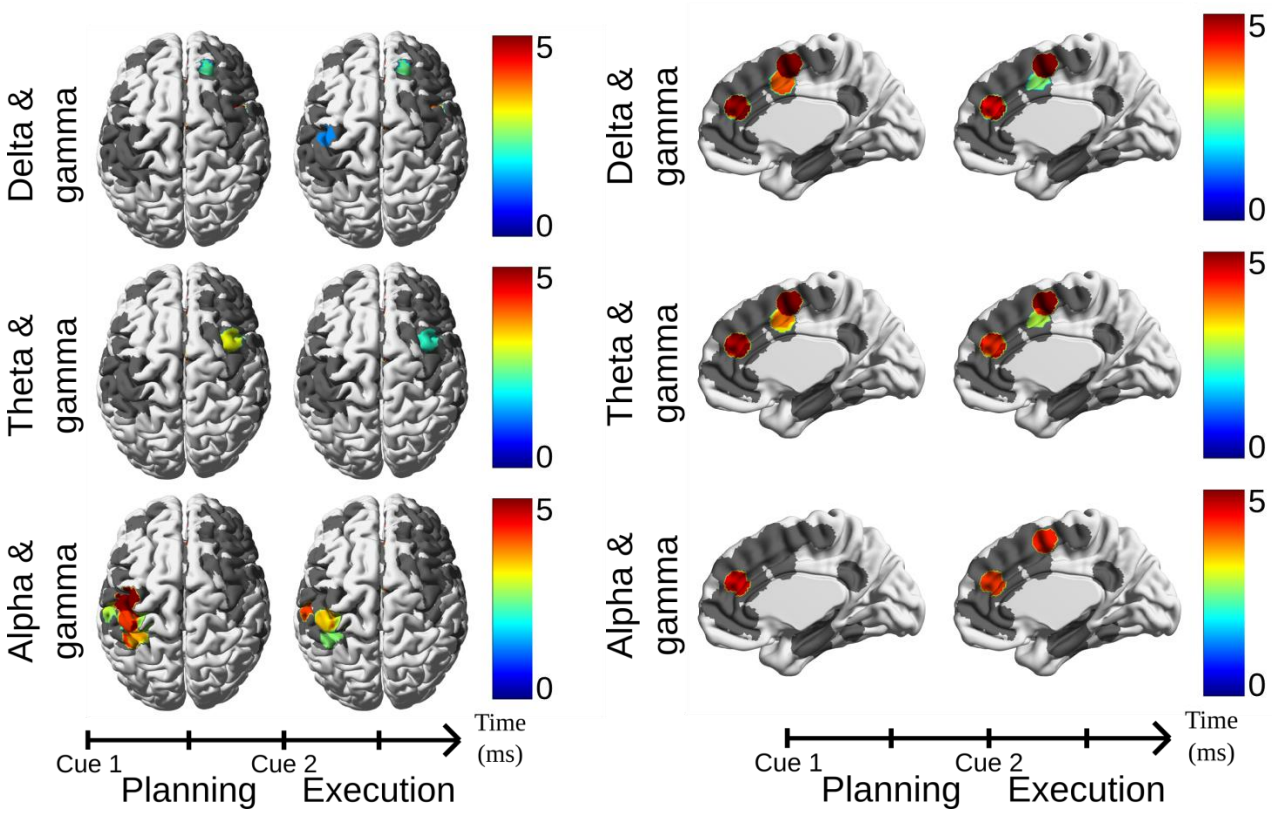

Figure 5. Task-related modulations of phase-amplitude coupling during planning and execution of upper limb movements (Left panel: top view, Right panel: medial view). The color bars represent mean PAC modulation index (MI) which quantifies the co-modulation of broadband gamma amplitude (60-200Hz) with delta (2-4Hz), theta (5-7Hz) and alpha (8-13Hz) bands. All modulations shown are statistically significant ($p<0.001$, surrogate data) and are estimated from the entire planning and execution time windows. Dark grey areas represent cortical regions for which electrode coverage was available but where the modulations did not reach statistical significance.

3.4 Single-trial decoding of motor processes using machine learning

The application of a supervised learning framework allowed us to determine which features, among those discussed above, provide single-trial decoding of motor states (binary classification applied pairwise to rest, planning and execution states). This was achieved using a cross-validation approach in which a classifier is repeatedly trained on a subset of the data and then tested on previously unseen single epoch observations (test set). This allows us to quantify the decoding strength of each feature as the percent correct classification rate.
The results in Fig 6 show the best decoding accuracies (DA) achieved with (on the x-axes) each feature type (power, phase and PAC) across all frequency bands, and (on the y-axes) all Brodmann areas for which recordings were available. The histograms above each panel depict the highest decoding accuracies obtained with each feature and indicate in which Brodmann area it was observed. The histograms on the right side of each panel indicate how many significant features were located in each Brodmann area. It is noteworthy that all features (amplitude, phase and PAC) computed across all frequencies and most of the probed brain areas all contain – to variable degrees- discriminant information on motor states (statistically significant decoding, $p<0.001$, permutation tests).

3.4.1 Classification similarities between Exec vs Rest and Intention vs Rest

The highest percentages of correct prediction were obtained when classifying Rest vs. Execution (as high as 99,4% on single-trial classifications). We found a high degree of similarity between the decoding patterns for Execution vs Rest (Fig 6A) and Intention vs Rest (Fig 6B). In principle, most of the features that provided significant decoding of execution vs Rest also provided significant decoding of Intention vs Rest. The features that yield the highest discrimination in both cases primarily involve spectral power in alpha (or mu), beta, low-gamma, and broadband gamma bands, in addition to phase in the very low frequency range (<1.5 Hz). The most prominent brain areas involved in both types of decoding are Brodmann areas 4, 6, 8, 9, 32 and 40. These were the regions that contained the highest number of significantly decoding sites (gray histograms), and these were also the Brodmann areas that yielded the highest levels of decoding accuracy. The highest DA performances reached 99,4% (Beta power in primary motor cortex) when decoding Execution vs Rest and 91,3% (VLFC phase in inferior parietal cortex, BA40) in the case of Intention vs Rest.

3.4.2 Classification differences between Exec vs Rest and Intention vs Rest

Although the decoding matrices in Figs 6A and 6B show a high degree of similarity, there are noteworthy differences. Brodmann area 40 plays a more prominent role in distinguishing intention from rest than actual movement execution from rest. This is in line with the role of inferior parietal lobe in motor planning (Caspers et al., 2008; Mattingley et al., 1998; Rushworth et al., 2001) Interestingly the involvement of BA40 was manifest in the phase and PAC features more than with power, although power in BA40 also provided statistically significant decoding (Fig 6B). In addition, power-based classification results show that while primary motor (BA4) and premotor areas (BA6) were prominent in predicting execution, the most noticeable intention-decoding power features were recorded from BA8, 9, 13 and 32 (Top histogram in Panel 6B). This is consistent with the previously reported involvement of BA8 and BA9 in working memory, executive planning and behavioral inhibition. Additionally, BA8 is also involved in visuomotor processing, visuospatial attention and motor imagery. The important decoding levels in BA13 could be related to the role of insular cortex, among other things, in motor planning (Lacourse et al., 2005; Stephan et al., 1995). Remarkably, the best PAC-mediated decoding of Intention vs Rest was obtained with delta-gamma coupling in the dorsal anterior cingulate cortex (dACC, BA32, DA=70%). This prominent PAC in ACC is consistent with the role of this area in motor inhibition, visuo spatial attention, motor

planning and imagery (Cheyne et al., 2012; Jahanshahi et al., 1995; Paus, 2001). To the best of our knowledge, this is the first report of a motor-related delta-gamma PAC modulation in ACC.

3.4.3 Classification of motor execution versus motor intention

The decoding matrix for Execution vs Intention (Fig 6C) shows a markedly different pattern. Because of the similarity between the neuronal responses in both conditions (cf. previous sections), the differences are subtle and, as a result, the decoding performances here are lower than those reported for the Execution vs Rest or Intention vs Rest classifications. In addition, fewer brain areas provide statistically significant decoding. Interestingly, among all features, the one that provided the best discrimination between the intention period and the execution period is the phase of the very low frequency range (<1.5 Hz), which yielded a decoding peak of 88,9% in BA 8. Interestingly, the second best decoding feature, after the low-frequency phase, was broadband gamma with a peak of decoding of (DA=83,5%) in posterior Insula (BA13). Moreover, although they did not provide the highest classifications performance, the premotor cortex sites (BA6) led to statistically significant decoding of intention vs execution with every single feature tested (peaking at 82,3% with VLFC phase). This is in line with the established involvement of premotor cortex in motor execution, planning and imagery, as well as visuomotor and visuospatial attention (Ball et al., 1999; Gallivan et al., 2013; Hanakawa et al., 2008; Miller et al., 2010). Finally, Figure 6C also shows that among all PAC features used, theta-gamma coupling provided the lowest decoding, while delta-gamma and alpha-gamma provided the best decoding, predominantly in primary motor (BA4) and premotor (BA6) cortices. This is most likely explained by the significant decoding accuracy (in these areas) of delta-gamma and alpha-gamma observed respectively in execution-rest (Fig 6A) and intention-rest (Fig 6B).

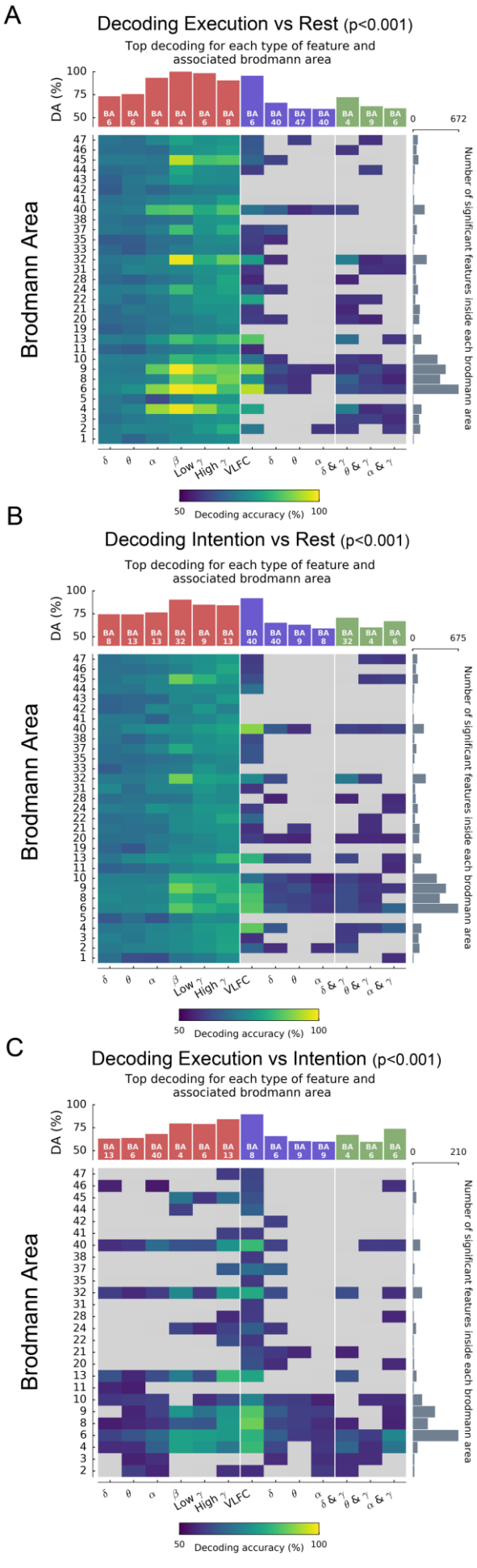
A
Decoding Execution vs Rest (p<0.001)
Top decoding for each type of feature and associated brodmann area
DA (%)
100
75
50
BA 6
BA 6
BA 4
BA 4
BA 6
BA 8
BA 6
BA 40
BA 47
BA 40
BA 4
BA 9
BA 6
0
672
Brodmann Area
Number of significant features inside each brodmann area
δ θ α β Low γ High γ VLFC δ θ α δ & γ θ & γ α & γ
50 Decoding accuracy (%) 100
B
Decoding Intention vs Rest (p<0.001)
Top decoding for each type of feature and associated brodmann area
DA (%)
BA 8
BA 13
BA 13
BA 32
BA 9
BA 13
BA 40
BA 40
BA 9
BA 8
BA 32
BA 4
BA 6
0
675
Brodmann Area
Number of significant features inside each brodmann area
δ θ α β Low γ High γ VLFC δ θ α δ & γ θ & γ α & γ
50 Decoding accuracy (%) 100
C
Decoding Execution vs Intention (p<0.001)
Top decoding for each type of feature and associated brodmann area
DA (%)
BA 13
BA 6
BA 40
BA 4
BA 6
BA 13
BA 8
BA 6
BA 9
BA 9
BA 4
BA 6
BA 6
0
210
Brodmann Area
Number of significant features inside each brodmann area
δ θ α β Low γ High γ VLFC δ θ α δ & γ θ & γ α & γ
50 Decoding accuracy (%) 100

Figure 6

Single-trial pairwise classification of motor states (pre-stimulus rest, intention and execution) using power, phase and PAC features. (**A**) Execution vs rest, (**B**) Intention vs rest (**C**) Execution vs intention. Each of the three decoding matrices depict the best percent decoding accuracies (DA) achieved with each feature type (power, phase and PAC) across all frequency bands (x-axes), and across all Brodmann areas for which recordings were available (y-axes). Yellow indicates 100% DA, while deep blue indicates 50% DA. Only statistically significant decoding accuracies are reported ($p<0.001$, permutation test). The bar plots above each panel show the highest decoding accuracies obtained with each feature (red: power, blue: phase and green: PAC) and indicate in which Brodmann area it was observed. The gray bar plots on the right side of each panel indicate how many significant features were located in each Brodmann area.

4 Discussion

4.1 Summary of findings

Previous reports have reported complex patterns of overlap and segregation between the networks of brain areas involved in action representation, planning and execution (e.g. Jeannerod, 1994; Stephan et al., 1995; Hanakawa et al., 2008; Guillot et al., 2012;) So far, electrophysiological explorations of these patterns in humans have focused on modulations of rhythmic activity, primarily measured through spectral power modulations. Using rare direct recordings in humans performing a delayed motor task, we here provide an intracranial investigation of the similarities and discrepancies between activations across areas involved in the build-up to action and those that actually mediate movement execution. To the best of our knowledge, this study provides the first account of the involved brain dynamics through systematic investigation of the roles of phase, amplitude and phase-amplitude coupling, measured in widely distributed brain areas (extending beyond primary motor areas) and across a wide range of frequencies (up to 200 Hz). Furthermore, in addition to statistical comparisons, an important addition of this study is the use of supervised learning and single-trial classification framework as a way to assess the distinct or overlapping information content of these features.

4.2 Planning and execution are associated with prominent phase, amplitude and PAC modulations

Our analyses of task-based modulations revealed spatially distributed patterns of statistically significant changes in power, phase and PAC, both during the delay period and following the execution cue. We found a large overlap between the patterns of significant modulations observed in the planning processes and in movement execution. In task-based power changes significant increases in the delta, theta and broadband gamma bands were present during the planning phase and further enhanced at the time of execution. By contrast, although largely present in the same areas, alpha, beta and low-gamma power showed a rather consistent pattern of inversion from increases following the preparation cue to decreases following the execution cue. These similarities and differences between activation patterns in intention and execution also echo previously reported similarities and differences when comparing motor imagery versus motor execution. In particular, action representation and motor inhibition are likely to be common to the delay period of the task used here and to motor imagery tasks (Stephan et al., 1995). Phase and PAC also displayed similar patterns of responses for action preparation and execution, although they also pinpointed to clear discrepancies in motor areas, such as prominent alpha-gamma coupling during planning, but delta-gamma coupling during execution. Although not spatially exhaustive, the reported pre- and peri-movement modulations of power, phase and PAC was found over large parts of parietal, frontal and prefrontal areas, including medial areas such as the dACC. Although, the reported power modulations are largely consistent with previous iEEG reports (Crone, 1998; Crone et al., 2006, 1998; Pfurtscheller and Lopes da Silva, 1999), the wide-spread significant modulations of phase and PAC effects, during the delay-period and movement execution, are to our knowledge novel findings that extend the current understanding of their role in mediating motor behavior (cf.. Yanagisawa et al., 2012).

4.3 Decoding patterns reveal functional overlap and discrepancies across phase, amplitude and PAC

The machine learning framework allowed a second level of investigation of the role of the explored features through the assessment of their decoding accuracy. Most importantly, the classification strategy extends the standard statistical analyses by switching from comparisons of means to evaluating the predictive power of data computed from single-trials; once trained, the classifier is individually applied to each single-trial of the test set. In other words, the mean decoding performances reflect the ability of each feature to discriminate between the classes (rest, intention, execution) on single samples of data. Taken together, the decoding analyses provide a rich multi-dimensional exploration of the functional involvement of the phase, amplitude and phase-amplitude in motor behavior. The main findings can be summarized as follows: First of all, they reveal a prominent role for slow frequency phase primarily in inferior parietal areas (up to DA>90%) and phase-amplitude coupling in dACC (up to DA>70%) during the delay-period preceding motor execution. Second, in contrast to classification in the planning phase, the highest classification accuracies for movement execution were achieved by power features rather than phase, and the best accuracies were found predominantly in sites in motor and premotor areas (BA4, 6 and 8). While during planning, the best power-based decoding levels were observed in prefrontal regions (BA8, 9, 13 and 32). Thirdly, we show that when it comes to directly distinguishing the neuronal correlates of execution from those mediating intention the highest classifications (among all explored regions) were achieved either with the phase of the very low frequency range (<1.5 Hz) in BA8 (DA>88%) or broadband gamma (60-200 Hz) power posterior Insula (DA>83%).

4.4 Relationship with previous electrophysiological findings in humans

Overall, the present analysis of invasive human data provides strong evidence for a prominent role of phase and phase-amplitude relationships in motor goal encoding and execution. These findings extend previous invasive electrophysiological studies in human that have investigated the correlates of motor intention and/or execution. For the large part, such studies are primarily based on the estimation of cortical power modulations in multiple frequency components of the local-field potential (LFP). Nevertheless, there is some evidence by a few studies that suggests a critical role for low-frequency phase and amplitude information in mediating movement parameters (Hammer et al., 2016, 2013; Jerbi et al., 2011, 2007; Milekovic et al., 2012; Miller et al., 2012; Waldert et al., 2009, 2008; (Kajihara et al., 2015; Liu et al., 2011) . Using ECoG recordings in epielpsy patients, (Hammer et al., 2013) directly addressed the role of phase information in decoding movement kinematics (i.e. position, velocity, and acceleration). By separately exploring kinematics decoding with spectral amplitudes and phase of the low frequency component (LFC), the authors came to the conclusion that the ECoG LFC phase is indeed much more informative than amplitudes (Hammer et al., 2013). Interestingly, a recent study by the same group has demonstrated that the LFC signal is more adapted to speed then to velocity decoding (Hammer et al., 2016). These findings are globally in line with reports of low fequency range coherence (<4 Hz) between limb speed and the activity of the primary motor cortex during continuous movements (Jerbi et al., 2007). Moreover, movement direction classification has also been achieved with significant success using the LFC component both with invasive and non-invasive brain recordings (Jerbi et al., 2011; Waldert et al., 2009, 2008).

The results of the current study differ from the above reports in several ways. First of all, while most studies typically focus on movement execution, the delayed-motor task used here allowed us to examine the role of phase information in the motor encoding and planning phase preceding actual movement execution. Secondly, beyond phase or amplitude, we performed a systematic exploration of phase-amplitude coupling effects and found that it yielded significant modulations and motor

state decoding. Thirdly, the intracerebral recordings used here provide a different spatial sampling compared to most previous electrocorticographic studies. In particular, the recording sites used here cover widely distributed brain areas beyond primary and secondary motor areas (such as parietal, prefrontal and insular cortices) and include some medial brain areas (e.g. dACC). Our rare exploration confirms and extends the growing body of evidence for the role of phase and phase-related measures in encoding motor processes along the path from intention to execution.

4.5 A key role for phase coding in goal-directed motor behavior

The overwhelming body of current research on the oscillatory brain dynamics that mediate motor behavior, continues to explore local activations in terms of amplitude modulations, while phase information is predominantly employed in the context of inter-regional connectivity assessments (da Silva, 2006; Lachaux et al., 1999; Le Van Quyen et al., 2001; Roach and Mathalon, 2008). Our findings support the view that phase carries critical information that is often overlooked and which, as shown here, can actually provide more task-specific information than spectral amplitude. One may thus ask what is the underlying physiological phenomenon that may explain the relevance of phase? One potential explanation is that phase modulations may be closely related to neuronal firing patterns. Evidence for this hypothesis has been found in non-human primates, for instance in auditory and visual cortices (Ng et al., 2013; Montemurro et al., 2008). In auditory cortex, stimulus selective firing patterns were found to imprint on the phase rather than the amplitude of theta oscillations both in LFPs and EEG data (Ng et al. 2013). By applying a stimulus decoding technique to intracortical LFPs and single cell recordings in macaque auditory cortex, the authors found that the stimuli which were successfully discriminated by firing rates were also discriminated by phase patterns but not by oscillation amplitude. In visual cortex, information theoretical approaches have also shown that spikes and low frequency (1-4 Hz) LFP phase provide, when combined, more information on visual stimuli than that achieved with spikes alone (Latham and Lengyel, 2008; Montemurro et al., 2008). In the hippocampus, the timing of action potentials relative to LFP theta phase has been shown to provide information about position with higher precision than what could be inferred from the firing rate alone (Dragoi and Buzsáki, 2006; O'Keefe and Recce, 1993).

The low-frequency phase decoding results obtained in the current study could in theory be explained by (and be consistent with) the hypothesis that the precise relationship between slow LFP phase and neuronal firing reported in other modalities (as discussed above) also operates in human motor brain areas during limb movement preparation and execution. This needs to be tested with microelectrode data allowing for simultaneous access to LFP and neuronal firing in humans. This was not possible with the SEEG data used for the purpose of this study. Furthermore, the significant modulations and decoding results reported here using phase-amplitude coupling, could suggest a specific mechanism by which phase, broadband gamma amplitude and neuronal firing are precisely lined up. Whittingstall and Logothetis (2009) observed such a phenomenon in Macaque visual cortex, where multi-unit firing responses were found to be strongest only when increases in EEG gamma power occurred during a specific phase of the delta (2-4 Hz) wave. Obviously, the tempting speculation that this may also be at play in areas where we found significant PAC decoding cannot be confirmed without simultaneous monitoring of neuronal firing.

Although the notion of phase coding *per se* is of course not new, the results found here extend an emerging body of literature that indicates that phase coding may play a more important role in motor behavior than previously admitted. In particular, we found that phase-based motor state decoding is (i) widely distributed, extending beyond primary motor areas, (ii) that it occurs both during action planning and execution, and (iii) that phase-amplitude coupling could be an additional phase-based key feature involved in the neuronal coding of goal-directed behavior.

4.6 Limitations and open questions

The results reported here have a number of limitations. As in all previous intracranial EEG studies, only limited spatial sampling of the involved networks is possible. The over 500 intracerebral sites used here only provide partial spatial coverage of the brain. This said the patients were selected primarily based on whether they had electrodes implanted in frontal, prefrontal or parietal areas, thus providing a reasonable coverage of the targeted networks. Moreover, as in all previous human invasive recordings, the participants suffer from drug-resistant epilepsy, which could limit the generalizability of the findings to healthy subjects. To address this in the best possible way, our standard procedure (e.g. Jerbi et al. 2009) is to exclude electrodes that display pathological activity (such as epileptic spikes) and to focus on task-related changes and multi-trial analyses thereby reducing the impact of neuronal activations that are not related to the task and which occur randomly across the recording session. Therefore, our findings would definitely benefit from future replication in non-invasive recordings with healthy controls. Furthermore, it is important to acknowledge that our task design did not allow for a fine-grained disambiguation of the various distinct processes that are expected to be at play in the delay period. Clearly, the delay period will encompass a wide range of processes such as stimulus encoding, visuomotor transformations, motor imagery, action selection, motor preparation as well as working memory and maintenance processes. To limit the bias towards visual stimulus encoding when analyzing the planning/intention period, we deliberately centered our phase and amplitude analyses on 500ms after target onset. However, more generally, this limitation will have to be addressed with a dedicated experimental design in future investigations. Moreover, the physiological interpretations made here also bare their share of limitations. The way the features explored here (amplitude, phase and PAC) explicitly relate to the notion of information processing in the human brain is still poorly understood. Rather than identifying the precise functional relevance of each feature, our results emphasize their task-specific modulations and their ability to successfully predict on singe-trial data the state of the system (i.e. rest, motor planning or motor execution).

Despite the above limitations, we feel that the rare access to intracerebral depth EEG recordings in human subjects, in particular with simultaneous monitoring of lateral and medial wall structures, provides a privileged access to the neural dynamics mediating human cognition with very high spatial, temporal and spectral precision. In the long run, such data can help bridge the gap with neuroimaging studies and with electrophysiological recordings in non-human primates.

5 Conclusion

The findings reported here provide novel experimental evidence for the role of oscillatory amplitude and phase properties in motor planning and execution. In particular, the evidence for phase and PAC-based coding provide compelling support for the key role of phase in encoding motor representations and mediating movement execution, across widely distributed brain areas. We hope that these results will pave the way for a better understanding and for novel hypotheses with respect to the role of phase, amplitude and the coordination between the two, in goal-directed motor behavior in humans.

Acknowledgments

Etienne Combrisson was supported in part by a PhD Scholarship awarded by the Ecole Doctorale Inter-Disciplinaire Sciences-Santé (EDISS), Lyon, France, and by PhD funding from the Natural Sciences and Engineering Research Council of Canada (NSERC). This work was partly performed within the framework of the LABEX CORTEX (ANR-11-LABX-0042) of Université de Lyon, within the program ANR-11-IDEX-0007 and thanks to funding from the Canada Research Chairs program and a Discovery Grant (RGPIN-2015-04854) awarded by the Natural Sciences and Engineering Research Council of Canada to K.J. The authors are grateful for the collaboration with patients and clinical staff at the Epilepsy Department of the Grenoble University Hospital.

Conflict of interest

The authors declare that there is no conflict of interests regarding the publication of this paper.

References

Ariani, G., Wurm, M.F., Lingnau, A., 2015. Decoding Internally and Externally Driven Movement Plans. J. Neurosci. Off. J. Soc. Neurosci. 35, 14160–14171. doi:10.1523/JNEUROSCI.0596-15.2015

Aru, J., Aru, J., Priesemann, V., Wibral, M., Lana, L., Pipa, G., Singer, W., Vicente, R., 2015. Untangling cross-frequency coupling in neuroscience. Curr. Opin. Neurobiol., SI: Brain rhythms and dynamic coordination 31, 51–61. doi:10.1016/j.conb.2014.08.002

Babiloni, C., Del Percio, C., Vecchio, F., Sebastiano, F., Di Gennaro, G., Quarato, P.P., Morace, R., Pavone, L., Soricelli, A., Noce, G., Esposito, V., Rossini, P.M., Gallese, V., Mirabella, G., 2016. Alpha, beta and gamma electrocorticographic rhythms in somatosensory, motor, premotor and prefrontal cortical areas differ in movement execution and observation in humans. Clin. Neurophysiol. Off. J. Int. Fed. Clin. Neurophysiol. 127, 641–654. doi:10.1016/j.clinph.2015.04.068

Babiloni, C., Babiloni, F., Carducci, F., Cincotti, F., Rosciarelli, F., Arendt-Nielsen, L., Chen, A.C.N., Rossini, P.M., 2002. Human brain oscillatory activity phase-locked to painful electrical stimulations: A multi-channel EEG study. Hum. Brain Mapp. 15, 112–123. doi:10.1002/hbm.10013

Bahramisharif, A., van Gerven, M.A.J., Aarnoutse, E.J., Mercier, M.R., Schwartz, T.H., Foxe, J.J., Ramsey, N.F., Jensen, O., 2013. Propagating Neocortical Gamma Bursts Are Coordinated by Traveling Alpha Waves. J. Neurosci. 33, 18849–18854. doi:10.1523/JNEUROSCI.2455-13.2013

Ball, T., Schreiber, A., Feige, B., Wagner, M., Lücking, C.H., Kristeva-Feige, R., 1999. The role of higher-order motor areas in voluntary movement as revealed by high-resolution EEG and fMRI. Neuroimage 10, 682–694.

Bastin, J., Deman, P., David, O., Gueguen, M., Benis, D., Minotti, L., Hoffman, D., Combrisson, E., Kujala, J., Perrone-Bertolotti, M., Kahane, P., Lachaux, J.-P., Jerbi, K., 2016. Direct Recordings from Human Anterior Insula Reveal its Leading Role within the Error-Monitoring Network. Cereb. Cortex bhv352. doi:10.1093/cercor/bhv352

Berens, P., others, 2009. CircStat a MATLAB toolbox for circular statistics. J Stat Softw 31, 1–21.

Brovelli, A., Lachaux, J.-P., Kahane, P., Boussaoud, D., 2005. High gamma frequency oscillatory activity dissociates attention from intention in the human premotor cortex. NeuroImage 28, 154–164. doi:10.1016/j.neuroimage.2005.05.045

Bundy, D.T., Pahwa, M., Szrama, N., Leuthardt, E.C., 2016. Decoding three-dimensional reaching movements using electrocorticographic signals in humans. J. Neural Eng. 13, 026021. doi:10.1088/1741-2560/13/2/026021

Canolty, R.T., 2006. High Gamma Power Is Phase-Locked to Theta. science 1128115, 313.

Canolty, R. T., & Knight, R. T. (2010). The functional role of cross-frequency coupling. *Trends in Cognitive Sciences*, *14*(11), 506–515. http://doi.org/10.1016/j.tics.2010.09.001

Cheyne, D.O., Ferrari, P., Cheyne, J.A., 2012. Intended actions and unexpected outcomes: automatic and controlled processing in a rapid motor task. Front. Hum. Neurosci. 6, 237. doi:10.3389/fnhum.2012.00237

Cheyne, D., Bells, S., Ferrari, P., Gaetz, W., Bostan, A.C., 2008. Self-paced movements induce high-frequency gamma oscillations in primary motor cortex. NeuroImage 42, 332–342. doi:10.1016/j.neuroimage.2008.04.178

Cohen, M.X., Elger, C.E., Fell, J., 2008. Oscillatory activity and phase–amplitude coupling in the human medial frontal cortex during decision making. J. Cogn. Neurosci. 21, 390–402.

Combrisson, E., Jerbi, K., 2015. Exceeding chance level by chance: The caveat of theoretical chance levels in brain signal classification and statistical assessment of decoding accuracy. J. Neurosci. Methods 250, 126–136. doi:10.1016/j.jneumeth.2015.01.010

Crone, N., 1998. Functional mapping of human sensorimotor cortex with electrocorticographic spectral analysis. I. Alpha and beta event- related desynchronization. Brain 121, 2271–2299. doi:10.1093/brain/121.12.2271

Crone, N.E., Miglioretti, D.L., Gordon, B., Lesser, R.P., 1998. Functional mapping of human sensorimotor cortex with electrocorticographic spectral analysis. II. Event-related synchronization in the gamma band. Brain 121, 2301–2315.

Crone, N.E., Sinai, A., Korzeniewska, A., 2006. High-frequency gamma oscillations and human brain mapping with electrocorticography, in: Progress in Brain Research. Elsevier, pp. 275–295.

da Silva, F.H.L., 2006. Event-related neural activities: what about phase? Prog. Brain Res. 159, 3–17.

Desmurget, M., Sirigu, A., 2009. A parietal-premotor network for movement intention and motor awareness. Trends Cogn. Sci. 13, 411–419. doi:10.1016/j.tics.2009.08.001

Dragoi, G., Buzsáki, G., 2006. Temporal Encoding of Place Sequences by Hippocampal Cell Assemblies. Neuron 50, 145–157. doi:10.1016/j.neuron.2006.02.023

Drewes, J., VanRullen, R., 2011. This Is the Rhythm of Your Eyes: The Phase of Ongoing Electroencephalogram Oscillations Modulates Saccadic Reaction Time. J. Neurosci. 31, 4698–4708. doi:10.1523/JNEUROSCI.4795-10.2011

Dugue, L., Marque, P., VanRullen, R., 2011. The Phase of Ongoing Oscillations Mediates the Causal Relation between Brain Excitation and Visual Perception. J. Neurosci. 31, 11889–11893. doi:10.1523/JNEUROSCI.1161-11.2011

Foster, B.L., Parvizi, J., 2012. Resting oscillations and cross-frequency coupling in the human posteromedial cortex. NeuroImage 60, 384–391. doi:10.1016/j.neuroimage.2011.12.019

Gallivan, J.P., McLean, D.A., Flanagan, J.R., Culham, J.C., 2013. Where one hand meets the other: limb-specific and action-dependent movement plans decoded from preparatory signals in single human frontoparietal brain areas. J. Neurosci. 33, 1991–2008.

Golland, P., Fischl, B., 2003. Permutation tests for classification: towards statistical significance in image-based studies. Inf. Process. Med. Imaging Proc. Conf. 18, 330–341.

Guillot, A., Di Rienzo, F., MacIntyre, T., Moran, A., Collet, C., 2012. Imagining is not doing but involves specific motor commands: a review of experimental data related to motor inhibition. Front. Hum. Neurosci. 6, 247.

Hammer, J., Fischer, J., Ruescher, J., Schulze-Bonhage, A., Aertsen, A., Ball, T., 2013. The role of ECoG magnitude and phase in decoding position, velocity, and acceleration during continuous motor behavior. Front. Neurosci. 7. doi:10.3389/fnins.2013.00200

Hammer, J., Pistohl, T., Fischer, J., Kršek, P., Tomášek, M., Marusič, P., Schulze-Bonhage, A., Aertsen, A., Ball, T., 2016. Predominance of Movement Speed Over Direction in Neuronal Population Signals of Motor Cortex: Intracranial EEG Data and A Simple Explanatory Model. Cereb. Cortex 26, 2863–2881. doi:10.1093/cercor/bhw033

Hanakawa, T., Dimyan, M.A., Hallett, M., 2008. Motor Planning, Imagery, and Execution in the Distributed Motor Network: A Time-Course Study with Functional MRI. Cereb. Cortex 18, 2775–2788. doi:10.1093/cercor/bhn036

Hemptinne, C. de, Ryapolova-Webb, E.S., Air, E.L., Garcia, P.A., Miller, K.J., Ojemann, J.G., Ostrem, J.L., Galifianakis, N.B., Starr, P.A., 2013. Exaggerated phase–amplitude coupling in the primary motor cortex in Parkinson disease. Proc. Natl. Acad. Sci. doi:10.1073/pnas.1214546110

Hyafil, A., Giraud, A.-L., Fontolan, L., Gutkin, B., 2015. Neural Cross-Frequency Coupling: Connecting Architectures, Mechanisms, and Functions. Trends Neurosci. 38, 725–740. doi:10.1016/j.tins.2015.09.001

Jahanshahi, M., Jenkins, I.H., Brown, R.G., Marsden, C.D., Passingham, R.E., Brooks, D.J., 1995. Self-initiated versus externally triggered movements. I. An investigation using measurement of regional cerebral blood flow with PET and movement-related potentials in normal and Parkinson's disease subjects. Brain J. Neurol. 118 (Pt 4), 913–933.

Jeannerod, M., 1994. The representing brain: Neural correlates of motor intention and imagery. Behav. Brain Sci. 17, 187–202.

Jensen, O., Colgin, L.L., 2007. Cross-frequency coupling between neuronal oscillations. Trends Cogn. Sci. 11, 267–269. doi:10.1016/j.tics.2007.05.003

Jensen, O., Gips, B., Bergmann, T.O., Bonnefond, M., 2014. Temporal coding organized by coupled alpha and gamma oscillations prioritize visual processing. Trends Neurosci. 37, 357–369. doi:10.1016/j.tins.2014.04.001

Jerbi, K., Lachaux, J.-P., Karim, N., Pantazis, D., Leahy, R.M., Garnero, L., Baillet, S., others, 2007. Coherent neural representation of hand speed in humans revealed by MEG imaging. Proc. Natl. Acad. Sci. 104, 7676–7681.

Jerbi, K., Ossandón, T., Hamamé, C.M., Senova, S., Dalal, S.S., Jung, J., Minotti, L., Bertrand, O., Berthoz, A., Kahane, P., Lachaux, J.-P., 2009. Task-related gamma-band dynamics from an intracerebral perspective: Review and implications for surface EEG and MEG. Hum. Brain Mapp. 30, 1758–1771. doi:10.1002/hbm.20750

Jerbi, K., Vidal, J.R., Mattout, J., Maby, E., Lecaignard, F., Ossandon, T., Hamamé, C.M., Dalal, S.S., Bouet, R., Lachaux, J.-P., Leahy, R.M., Baillet, S., Garnero, L., Delpuech, C., Bertrand, O., 2011. Inferring hand movement kinematics from MEG, EEG and intracranial EEG: From brain-machine interfaces to motor rehabilitation. IRBM 32, 8–18. doi:10.1016/j.irbm.2010.12.004

Jerbi, K., Vidal, J.R., Ossandon, T., Dalal, S.S., Jung, J., Hoffmann, D., Minotti, L., Bertrand, O., Kahane, P., Lachaux, J.-P., 2010. Exploring the electrophysiological correlates of the default-mode network with intracerebral EEG. Front. Syst. Neurosci. 4, 27. doi:10.3389/fnsys.2010.00027

Jurkiewicz, M.T., Gaetz, W.C., Bostan, A.C., Cheyne, D., 2006. Post-movement beta rebound is generated in motor cortex: Evidence from neuromagnetic recordings. NeuroImage 32, 1281–1289. doi:10.1016/j.neuroimage.2006.06.005

Kahane, P., Landré, E., Minotti, L., Francione, S., Ryvlin, P., 2006. The Bancaud and Talairach view on the epileptogenic zone: a working hypothesis. Epileptic Disord. Int. Epilepsy J. Videotape 8, S16–26.

Kajihara, T., Anwar, M.N., Kawasaki, M., Mizuno, Y., Nakazawa, K., Kitajo, K., 2015. Neural dynamics in motor preparation: From phase-mediated global computation to amplitude-mediated local computation. NeuroImage 118, 445–455. doi:10.1016/j.neuroimage.2015.05.032

Kalaska, J.F., 2009. From Intention to Action: Motor Cortex and the Control of Reaching Movements, in: Sternad, D. (Ed.), Progress in Motor Control. Springer US, Boston, MA, pp. 139–178.

Klimesch, W., Freunberger, R., Sauseng, P., Gruber, W., 2008. A short review of slow phase synchronization and memory: Evidence for control processes in different memory systems? Brain Res., Brain Oscillations in Cognition and Cognitive Disorders 1235, 31–44. doi:10.1016/j.brainres.2008.06.049

Klimesch, W., Sauseng, P., Hanslmayr, S., 2007. EEG alpha oscillations: The inhibition–timing hypothesis. Brain Res. Rev. 53, 63–88. doi:10.1016/j.brainresrev.2006.06.003

Lachaux, J.-P., Rodriguez, E., Martinerie, J., Varela, F.J., others, 1999. Measuring phase synchrony in brain signals. Hum. Brain Mapp. 8, 194–208.

Lachaux, J.P., Rudrauf, D., Kahane, P., 2003. Intracranial EEG and human brain mapping. J. Physiol.-Paris 97, 613–628. doi:10.1016/j.jphysparis.2004.01.018

Lacourse, M.G., Orr, E.L.R., Cramer, S.C., Cohen, M.J., 2005. Brain activation during execution and motor imagery of novel and skilled sequential hand movements. NeuroImage 27, 505–519. doi:10.1016/j.neuroimage.2005.04.025

Lakatos, P., 2005. An Oscillatory Hierarchy Controlling Neuronal Excitability and Stimulus Processing in the Auditory Cortex. J. Neurophysiol. 94, 1904–1911. doi:10.1152/jn.00263.2005

Latham, P.E., Lengyel, M., 2008. Phase Coding: Spikes Get a Boost from Local Fields. Curr. Biol. 18, R349–R351. doi:10.1016/j.cub.2008.02.062

Lau, H.C., 2004. Attention to Intention. Science 303, 1208–1210. doi:10.1126/science.1090973

Le Van Quyen, M., Foucher, J., Lachaux, J.-P., Rodriguez, E., Lutz, A., Martinerie, J., Varela, F.J., 2001. Comparison of Hilbert transform and wavelet methods for the analysis of neuronal synchrony. J. Neurosci. Methods 111, 83–98.

Lee, J., Jeong, J., 2013. Correlation of risk-taking propensity with cross-frequency phase–amplitude coupling in the resting EEG. Clin. Neurophysiol. doi:10.1016/j.clinph.2013.05.007

Lemm, S., Blankertz, B., Dickhaus, T., Müller, K.-R., 2011. Introduction to machine learning for brain imaging. NeuroImage 56, 387–399. doi:10.1016/j.neuroimage.2010.11.004

Liu, J., Perdoni, C., He, B., 2011. Hand movement decoding by phase-locking low frequency EEG signals. Conf. Proc. Annu. Int. Conf. IEEE Eng. Med. Biol. Soc. IEEE Eng. Med. Biol. Soc. Annu. Conf. 2011, 6335–6338. doi:10.1109/IEMBS.2011.6091564

Meyers, E., Kreiman, G., 2012. Tutorial on pattern classification in cell recording. Vis. Popul. Codes 517–538.

Milekovic, T., Fischer, J., Pistohl, T., Ruescher, J., Schulze-Bonhage, A., Aertsen, A., Rickert, J., Ball, T., Mehring, C., 2012. An online brain–machine interface using decoding of movement direction from the human electrocorticogram. J. Neural Eng. 9, 046003. doi:10.1088/1741-2560/9/4/046003

Miller, K.J., Schalk, G., Fetz, E.E., den Nijs, M., Ojemann, J.G., Rao, R.P., 2010. Cortical activity during motor execution, motor imagery, and imagery-based online feedback. Proc. Natl. Acad. Sci. 107, 4430–4435.

Miller, K.J., Hermes, D., Honey, C.J., Hebb, A.O., Ramsey, N.F., Knight, R.T., Ojemann, J.G., Fetz, E.E., 2012. Human Motor Cortical Activity Is Selectively Phase-Entrained on Underlying Rhythms. PLoS Comput. Biol. 8, e1002655. doi:10.1371/journal.pcbi.1002655

Montemurro, M.A., Rasch, M.J., Murayama, Y., Logothetis, N.K., Panzeri, S., 2008. Phase-of-Firing Coding of Natural Visual Stimuli in Primary Visual Cortex. Curr. Biol. 18, 375–380. doi:10.1016/j.cub.2008.02.023

Nakhnikian, A., Ito, S., Dwiel, L.L., Grasse, L.M., Rebec, G.V., Lauridsen, L.N., Beggs, J.M., 2016. A novel cross-frequency coupling detection method using the generalized Morse wavelets. J. Neurosci. Methods 269, 61–73. doi:10.1016/j.jneumeth.2016.04.019

Newman, E.L., Gillet, S.N., Climer, J.R., Hasselmo, M.E., 2013. Cholinergic Blockade Reduces Theta-Gamma Phase Amplitude Coupling and Speed Modulation of Theta Frequency Consistent with Behavioral Effects on Encoding. J. Neurosci. 33, 19635–19646. doi:10.1523/JNEUROSCI.2586-13.2013

Ng, B.S.W., Logothetis, N.K., Kayser, C., 2013. EEG Phase Patterns Reflect the Selectivity of Neural Firing. Cereb. Cortex 23, 389–398. doi:10.1093/cercor/bhs031

O'Keefe, J., Recce, M.L., 1993. Phase relationship between hippocampal place units and the EEG theta rhythm. Hippocampus 3, 317–330.

Ojala, M., Garriga, G.C., 2010. Permutation tests for studying classifier performance. J. Mach. Learn. Res. 11, 1833–1863.

Ossandon, T., Jerbi, K., Vidal, J.R., Bayle, D.J., Henaff, M.-A., Jung, J., Minotti, L., Bertrand, O., Kahane, P., Lachaux, J.-P., 2011. Transient Suppression of Broadband Gamma Power in the Default-Mode Network Is Correlated with Task Complexity and Subject Performance. J. Neurosci. 31, 14521–14530. doi:10.1523/JNEUROSCI.2483-11.2011

Ossandon, T., Vidal, J.R., Ciumas, C., Jerbi, K., Hamame, C.M., Dalal, S.S., Bertrand, O., Minotti, L., Kahane, P., Lachaux, J.-P., 2012. Efficient "Pop-Out" Visual Search Elicits Sustained Broadband Gamma Activity in the Dorsal Attention Network. J. Neurosci. 32, 3414–3421. doi:10.1523/JNEUROSCI.6048-11.2012

Ozkurt, T.E., 2012. Statistically Reliable and Fast Direct Estimation of Phase-Amplitude Cross-Frequency Coupling. Biomed. Eng. IEEE Trans. On 59, 1943–1950.

Özkurt, T.E., Schnitzler, A., 2011. A critical note on the definition of phase–amplitude cross-

frequency coupling. J. Neurosci. Methods 201, 438–443. doi:10.1016/j.jneumeth.2011.08.014
Palva, S., Palva, J.M., 2007. New vistas for α-frequency band oscillations. Trends Neurosci. 30, 150–158. doi:10.1016/j.tins.2007.02.001
Paus, T., 2001. Primate anterior cingulate cortex: where motor control, drive and cognition interface. Nat. Rev. Neurosci. 2, 417–424. doi:10.1038/35077500
Pfurtscheller, G., Lopes da Silva, F.H., 1999. Event-related EEG/MEG synchronization and desynchronization: basic principles. Clin. Neurophysiol. 110, 1842–1857.
Pfurtscheller, G., Graimann, B., Huggins, J.E., Levine, S.P., Schuh, L.A., 2003. Spatiotemporal patterns of beta desynchronization and gamma synchronization in corticographic data during self-paced movement. Clin. Neurophysiol. 114, 1226–1236. doi:10.1016/S1388-2457(03)00067-1
Pittman-Polletta, B., Hsieh, W.-H., Kaur, S., Lo, M.-T., Hu, K., 2014. Detecting phase-amplitude coupling with high frequency resolution using adaptive decompositions. J. Neurosci. Methods 226, 15–32. doi:10.1016/j.jneumeth.2014.01.006
Rektor, I., Sochůrková, D., Bocková, M., 2006. Intracerebral ERD/ERS in voluntary movement and in cognitive visuomotor task. Prog. Brain Res. 159, 311–330. doi:10.1016/S0079-6123(06)59021-1
Roach, B.J., Mathalon, D.H., 2008. Event-related EEG time-frequency analysis: an overview of measures and an analysis of early gamma band phase locking in schizophrenia. Schizophr. Bull. 34, 907–926.
Saleh, M., Reimer, J., Penn, R., Ojakangas, C.L., Hatsopoulos, N.G., 2010. Fast and Slow Oscillations in Human Primary Motor Cortex Predict Oncoming Behaviorally Relevant Cues. Neuron 65, 461–471. doi:10.1016/j.neuron.2010.02.001
Sauseng, P., Klimesch, W., 2008. What does phase information of oscillatory brain activity tell us about cognitive processes? Neurosci. Biobehav. Rev. 32, 1001–1013. doi:10.1016/j.neubiorev.2008.03.014
Schnitzler, A., Gross, J., 2005. Normal and pathological oscillatory communication in the brain. Nat. Rev. Neurosci. 6, 285–296. doi:10.1038/nrn1650
Schwartz, A.B., 2016. Movement: How the Brain Communicates with the World. Cell 164, 1122–1135. doi:10.1016/j.cell.2016.02.038
Sherman, M.T., Kanai, R., Seth, A.K., VanRullen, R., 2016. Rhythmic Influence of Top–Down Perceptual Priors in the Phase of Prestimulus Occipital Alpha Oscillations. J. Cogn. Neurosci.
Snyder, L.H., Batista, A.P., Andersen, R.A., 1997. Coding of intention in the posterior parietal cortex. Nature 386, 167–170. doi:10.1038/386167a0
Soto, J.L., Jerbi, K., 2012. Investigation of cross-frequency phase-amplitude coupling in visuomotor networks using magnetoencephalography, in: Engineering in Medicine and Biology Society (EMBC), 2012 Annual International Conference of the IEEE. IEEE, pp. 1550–1553.
Stephan, K.M., Fink, G.R., Passingham, R.E., Silbersweig, D., Ceballos-Baumann, A.O., Frith, C.D., Frackowiak, R.S., 1995. Functional anatomy of the mental representation of upper extremity movements in healthy subjects. J. Neurophysiol. 73, 373–386.
Talairach, J., Tournoux, P., 1993. Referentially oriented cerebral MRI anatomy: an atlas of stereotaxic anatomical correlations for gray and white matter. Thieme.
Tallon-Baudry, C., Bertrand, O., Delpuech, C., Pernier, J., 1996. Stimulus specificity of phase-locked and non-phase-locked 40 Hz visual responses in human. J. Neurosci. 16, 4240–4249.
Tort, A.B.L., Komorowski, R., Eichenbaum, H., Kopell, N., 2010. Measuring Phase-Amplitude Coupling Between Neuronal Oscillations of Different Frequencies. J. Neurophysiol. 104, 1195–1210. doi:10.1152/jn.00106.2010
VanRullen, R., Busch, N., Drewes, J., Dubois, J., 2011. Ongoing EEG Phase as a Trial-by-Trial Predictor of Perceptual and Attentional Variability. Front. Psychol. 2, 60.
Voytek, B., 2010. Shifts in gamma phase–amplitude coupling frequency from theta to alpha over

posterior cortex during visual tasks. Front. Hum. Neurosci. 4. doi:10.3389/fnhum.2010.00191

Voytek, B., D'Esposito, M., Crone, N., Knight, R.T., 2013. A method for event-related phase/amplitude coupling. NeuroImage 64, 416–424. doi:10.1016/j.neuroimage.2012.09.023

Waldert, S., Pistohl, T., Braun, C., Ball, T., Aertsen, A., Mehring, C., 2009. A review on directional information in neural signals for brain-machine interfaces. J. Physiol.-Paris 103, 244–254. doi:10.1016/j.jphysparis.2009.08.007

Waldert, S., Preissl, H., Demandt, E., Braun, C., Birbaumer, N., Aertsen, A., Mehring, C., 2008. Hand Movement Direction Decoded from MEG and EEG. J. Neurosci. 28, 1000–1008. doi:10.1523/JNEUROSCI.5171-07.2008

Whittingstall, K., Logothetis, N.K., 2009. Frequency-Band Coupling in Surface EEG Reflects Spiking Activity in Monkey Visual Cortex. Neuron 64, 281–289. doi:10.1016/j.neuron.2009.08.016

Yanagisawa, T., Yamashita, O., Hirata, M., Kishima, H., Saitoh, Y., Goto, T., Yoshimine, T., Kamitani, Y., 2012. Regulation of Motor Representation by Phase–Amplitude Coupling in the Sensorimotor Cortex. J. Neurosci. 32, 15467–15475. doi:10.1523/JNEUROSCI.2929-12.2012